INTERACTIONS OF SOLITARY WAVES IN HIERARCHICAL KdV-TYPE SYSTEM
Research Report Mech 291/08

Lauri Ilison, Andrus Salupere

Centre for Nonlinear Studies, Institute of Cybernetics at Tallinn University of Technology, Akadeemia tee 21, 12618, Tallinn, Estonia

Abstract

In the present paper a hierarchical Korteweg–de Vries type evolution equation is applied for modelling interactions of propagating solitary waves in dilatant granular materials. The model equation is integrated numerically under sech^2-type initial conditions making use of the Fourier transform based pseudospectral method. Analysis of the interactions bases on the solution types defined in [1]. The main goal is to examine the character of solution in the terms of solitons, i.e. to understand whether or no solitary waves that emerge from different initial pulses interact elastically.

Key words: Korteweg–de Vries type evolution equations, Solitons, Wave hierarchies, Dilatant granular materials
PACS: 05.45.Yv

1 Introduction

Many physical and engineering applications lead to the problem of nonlinear waves propagating in media that can be modelled as continua with microstructure. For that reason corresponding studies have seen increased attention in recent years (see e.g. [2–4] and references therein). ¿From the viewpoint of wave propagation the most important characteristics of microstructured materials are intrinsic space-scales like the size of grain or a crystallite, the lattice period, the distance between the microcracks, etc. which introduce the scale dependence into the governing equations. Granular materials are an example

Email addresses: lauri@cens.ioc.ee (Lauri Ilison), salupere@ioc.ee (Andrus Salupere).

of such microstructured materials [5–8]. In studying the dynamics of granular materials the most important scale factor is an averaged diameter of a grain that must be related to the wavelength of the excitation (i.e. propagating wave). The scale-dependence involves dispersive as well as nonlinear effects and if these two effects are balanced then solitary waves and solitons can exist in such media.

In the present paper we simulate interactions of propagating solitary waves in dilatant granular materials making use of a model equation, which is derived by Giovine and Oliveri [5]. This model considers the suspension of grains (particles) in a compressible fluid with fluid density assumed to be small compared to the particle density. In addition, the rotation of particles is neglected. It is demonstrated that in case of compressible grains 1D equations of motion result in a hierarchical Korteweg–de Vries (HKdV) equation

$$\frac{\partial u}{\partial t} + u\frac{\partial u}{\partial x} + \alpha_1 \frac{\partial^3 u}{\partial x^3} + \beta \frac{\partial^2}{\partial x^2}\left(\frac{\partial u}{\partial t} + u\frac{\partial u}{\partial x} + \alpha_2 \frac{\partial^3 u}{\partial x^3}\right) = 0. \tag{1}$$

Here the variable u is bulk density, α_1, α_2 are macro- and microlevel dispersion parameters, respectively, and β is a parameter involving the ratio of the grain size and the wavelength. The parameter β can be negative or positive depending on the ratio of kinetic and potential energies of particles [5]. It is obvious, that equation (1) involves two Korteweg–de Vries (KdV) operators — the first describes motion in the macrostructure and the second (within the brackets) accounts for motion in the microstructure — and parameter β controls the influence of the microstructure. Therefore equation (1) is clearly hierarchical in the Whitham's sense [9]. The limiting case ($\beta = 0$) results in the standard KdV equation with standard soliton solutions.

On the other hand the HKdV equation includes a fifth order dispersive term and complicated nonlinear terms and can therefore be considered as a higher order KdV-type equation. During recent years KdV-type equations with higher order dispersive and/or nonlinear terms have been studied by many authors. For example, a compaction solution is found for the modified KdV equation making use of Adomian decomposition method [10]; the variable-coefficient generalized projected Ricatti equation expansion method is applied for finding exact solutions to the modified KdV equation with variable coefficients [11]; periodic wave trains and soliton-like solutions to the generalized KdV equation are found by using the extended mapping method [12]; the Bäcklund transform and Hirotas method have been applied in order to get analytical solutions for the fifth order KdV equation [13,14]; the propagation of sech^2-type localised pulses (KdV solitons) is simulated numerically in case of KdV-like evolution equation that includes both, the quartic nonlinear and the fifth-order dispersive terms [15,16]; a comparative study between two different methods (the numerical Crank Nicolson method, and the semi-analytic Adomian decomposition method) for solving the general KdV equation is carried out [17].

In our previous studies the HKdV equation (1) was solved numerically under localised initial conditions [1,18,19]. In these papers our main goal was to simulate emergence of solitons and soliton ensembles from a single sech^2-type initial pulse, which is an analytical solution of the KdV equation that corresponds to the first KdV operator in equation (1). Based on the analysis of numerical results we have demonstrated the existence of five different solution types: (i) Single KdV soliton, (ii) KdV soliton ensemble, (iii) KdV soliton ensemble with weak tail, (iv) Soliton with strong tail, and (v) Solitary wave (soliton) with tail and wave packet.

The main aim of this paper is to simulate and analyse interactions between the solitons and soliton ensembles that emerge from different sech^2-type initial pulses. In Section 2 the problem is stated and in Section 3 numerical technique is described. Numerical results are discussed in Section 4 while conclusions are drawn in Section 5.

2 Statement of the problem

In our previous papers [1,18,19] we have demonstrated, that solution type is determined by the values of material parameters α_1, α_2 and β irrespective to the value of the amplitude (height) A of the initial pulse. The latter only changes the propagation speed of emerged waves. Therefore two initial pulses having different amplitudes generate solitons that correspond to the same solution type but propagate at different speeds and therefore can interact during the propagation.

In order to simulate interactions between solitons and soliton ensembles we are using here an initial condition that consists of two sech^2-type localised waves which are shifted with the respect to $x = 0$ by 16π and 48π respectively:

$$
\begin{aligned}
&u(x,0) = A_1 \,\mathrm{sech}^2 \frac{x-16\pi}{\delta_1} + A_2 \,\mathrm{sech}^2 \frac{x-48\pi}{\delta_2},\\
&\delta_1 = \sqrt{\frac{12\alpha_1}{A_1}}, \qquad \delta_2 = \sqrt{\frac{12\alpha_1}{A_2}}.
\end{aligned}
\tag{2}
$$

Here A_1 is the amplitude of the left hand side and A_2 is the amplitude of the right hand side sech^2-type pulse, δ_1 and δ_2 are the widths of the initial pulses and $0 \le x < 64\pi$.

The goals of the present paper are:

(i) to simulate numerically interactions between

(a) two single KdV solitons (the first solution type in [1,18,19]);
(b) solitons from different KdV soliton ensembles (the second and the third solution types in [1,18,19]);
(c) two solitons with strong tails (the fourth solution type in [1,18,19]);
(d) two solitary waves with tails and wave packets (the fifth solution type in [1,18,19]);

(ii) to analyse the character of interactions in terms of solitons, i.e. to understand whether or no solitary waves that emerge from different initial pulses (which were defined to be solitons in [1,18,19]) interact elastically.

3 Numerical technique and stability of solutions

For numerical integration of the HKdV equation the pseudospectral method (PsM) [20–23] is applied. In a nutshell, the idea of the PsM is to approximate space derivatives by a certain global method — reducing thereby partial differential equation to ordinary differential equation (ODE) — and to apply a certain ODE solver for integration with respect to the time variable. In the present paper space derivatives are found making use of the discrete Fourier transform (DFT),

$$U(k,t) = Fu = \sum_{j=0}^{n-1} u(j\Delta x, t) \exp\left(-\frac{2\pi ijk}{n}\right), \tag{3}$$

where n is the number of space-grid points, $\Delta x = 2\pi/n$ space step, i imaginary unit, $k = 0, \pm 1, \pm 2, \ldots, \pm (n/2 - 1), -n/2$ and F denotes the DFT.

The usual PsM algorithm (derived for $u_t = \Phi(u, u_x, u_{2x}, \ldots, u_{nx})$ type equations) needs to be modified due to the existence of the mixed partial derivative in the HKdV equation (1). At first the HKdV equation is rewritten in the form

$$(u + \beta u_{2x})_t + (u + 3\beta u_{2x})\, u_x + (\alpha_1 + \beta u)\, u_{3x} + \beta\alpha_2 u_{5x} = 0 \tag{4}$$

and a variable

$$v = u + \beta u_{2x} \tag{5}$$

is introduced. Making use of the Fourier transform the last expression can be rewritten in the form

$$v = F^{-1}\left[F(u)\right] + \beta F^{-1}\left[-k^2 F(u)\right] = F^{-1}\left[\left(1 - \beta k^2\right) F(u)\right], \tag{6}$$

where F^{-1} denotes the inverse Fourier transform. ¿From the latter expression one can express the variable u and it's space derivatives in the terms of the new variable v:

$$u = F^{-1}\left[\frac{F(v)}{1-\beta k^2}\right], \qquad \frac{\partial^n u}{\partial x^n} = F^{-1}\left[\frac{(ik)^n F(v)}{1-\beta k^2}\right]. \tag{7}$$

Finally, equation (4) can be rewritten in terms of variable v

$$v_t = -(u + 3\beta u_{2x})u_x - (\alpha_1 + \beta u)\, u_{3x} - \alpha_2 \beta u_{5x}, \tag{8}$$

where variable u and all its space derivatives are calculated making use of formulae (7). Therefore equation (8) can be considered as an ODE with respect to the variable v and could be integrated numerically by standard ODE solvers.

Calculations are carried out using SciPy package [24], for DFT the FFTW [25] library and for ODE solver the F2PY [26] generated Python interface to ODEPACK Fortran code [27] is used.

The question about the stability and the accuracy of solutions certainly arises with any numerical computation. The studied HKdV equation (1) can be rewritten in the form of first conservation law

$$(u + \beta u_{2x})_t + \left[\frac{u^2}{2} + \alpha_1 u_{2x} + \beta(\frac{u^2}{2} + \alpha_2 u_{2x})_{2x}\right]_x = 0 \tag{9}$$

with conserved density

$$C_1(t) = \int\limits_0^{2\pi} (u + \beta u_{2x})\, dx \tag{10}$$

and in the form on second conservation law

$$\begin{aligned} &\left\{\frac{1}{2}\alpha_1 u^2 + \beta\left[(u_x)^2 + u u_{2x}\right]\right\}_t + \\ &\left\{\frac{1}{3}\alpha_1 u^3 + u u_{2x} - \frac{1}{2}(u_x)^2 + \beta\left[\frac{1}{3}\alpha_1 u^3 + u u_{2x} - \frac{1}{2}(u_x)^2\right]_{2x}\right\}_x = 0 \end{aligned} \tag{11}$$

with conserved density

$$C_2(t) = \int\limits_0^{2\pi} \left(\frac{1}{2}\alpha_1 u^2 + \beta\left[(u_x)^2 + u u_{2x}\right]\right) dx. \tag{12}$$

In order to estimate the accuracy of computations numerical experiments have been carried out with number of space-grid points $n = 2048, 4096, 8192$. The behavior of the conserved density was traced and final wave-profiles $u(x, t_f)$, i.e. the wave-profiles at the end of the integration interval $t = t_f$, were compared. It was found that final wave-profiles for $n \geq 4096$ practically coincide and therefore in numerical experiments below the number of space-grid points $n = 4096$ is used.

In all cases, discussed below, the relative error of the conserved density $C_1(t)$ is less than 10^{-10} and for $C_2(t)$ less than 10^{-2}.

4 Results and discussion

The HKdV equation (1) was integrated numerically under initial conditions (2) and periodic boundary conditions

$$u(x + 64k\pi, t) = u(x, t), \qquad k = \pm 1, \pm 2, \pm 3, \ldots. \tag{13}$$

The values of dispersion parameters α_1, α_2 and microstructure parameter β have been selected according to the solution types defined in [1,18,19]. The number of space grid points $n = 4096$ and the length of the time interval $t_f = 100$.

In the present paper we consider interactions for four solution types (defined in [1,18,19]):

(i) KdV solitons;
(ii) KdV soliton ensembles with weak tails;
(iii) Solitons with strong tails;
(iv) Solitary waves with tails and wave packets.

4.1 Interactions of single KdV solitons

The first solution type is called single KdV soliton and it appears if dispersion parameters $\alpha_1 = \alpha_2$. In this case the initial sech^2-pulse propagates at constant speed and constant amplitude [1,18,19].

Here we simulate interactions between two initial pulses that have different amplitudes and therefore they propagate at different speed. The left hand side solitary wave with amplitude $A_1 = 15$ propagates faster than the right hand side one with amplitude $A_1 = 5$ and interactions can take place (see corresponding time-slice, pseudocolor and amplitude plots in Figs. 1–3). This set of figures demonstrates clearly that interactions between solitons are elastic as the solitons restore their speeds and amplitudes after interactions. During the interaction solitons are phase shifted — higher amplitude soliton is shifted to the right and lower amplitude soliton to the left, see pseudocolor plot in Fig. 2.

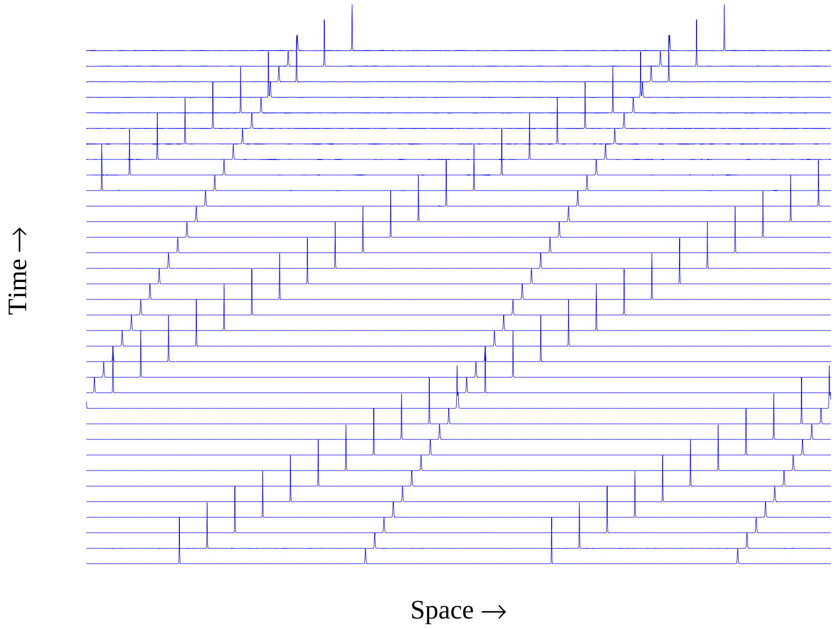

Fig. 1. Interactions of KdV solitons. Timeslice plot over two space periods for $\alpha_1 = \alpha_2 = 0.03$, $\beta = 0.0111$, $0 \leq t \leq 100$, $A_1 = 15$, $A_2 = 5$.

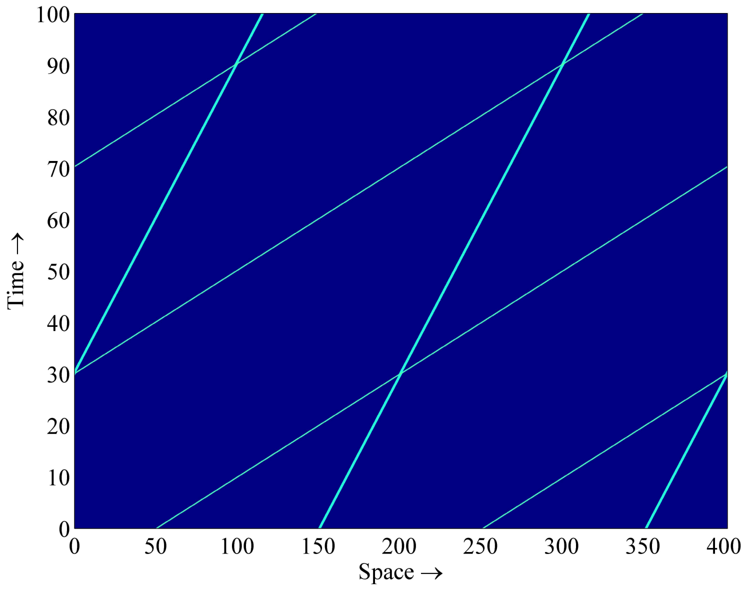

Fig. 2. Interactions of KdV solitons. Pseudocolor plot over two space periods for $\alpha_1 = \alpha_2 = 0.03$, $\beta = 0.0111$, $0 \leq t \leq 100$, $A_1 = 15$, $A_2 = 5$.

4.2 Interactions of solitons from KdV soliton ensembles with weak tails

In our previous papers [1,18,19] we found that it is quite conditional to distinguish between the second and the third solution types, i.e. between KdV

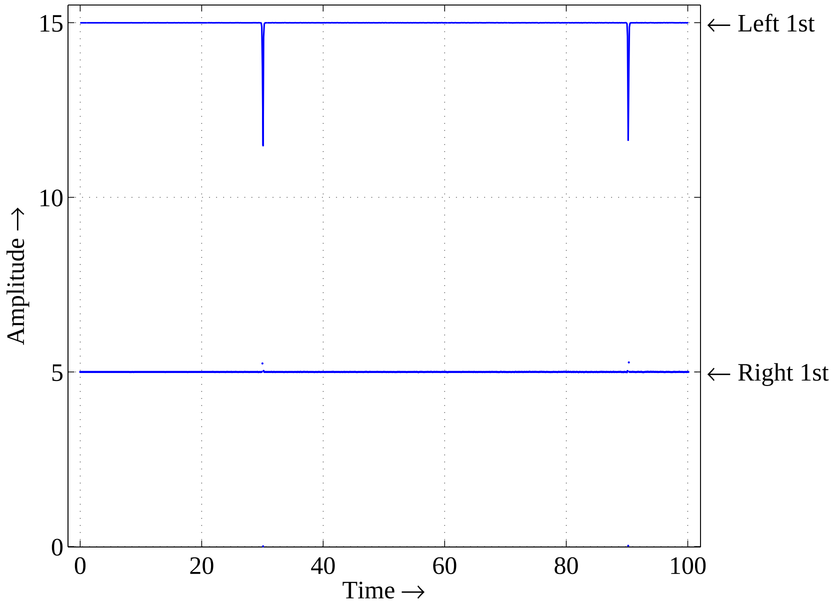

Fig. 3. Interactions of KdV solitons. Amplitudes of solitons against time in case of $\alpha_1 = \alpha_2 = 0.03$, $\beta = 0.0111$, $0 \leq t \leq 100$, $A_1 = 15$, $A_2 = 5$.

soliton ensemble and KdV soliton ensemble with a weak tail. The tail is sometimes so weak, that it is practically indistinguishable by means of wave profile extrema as well as spectral quantities. For this reason we consider here these two solution types together.

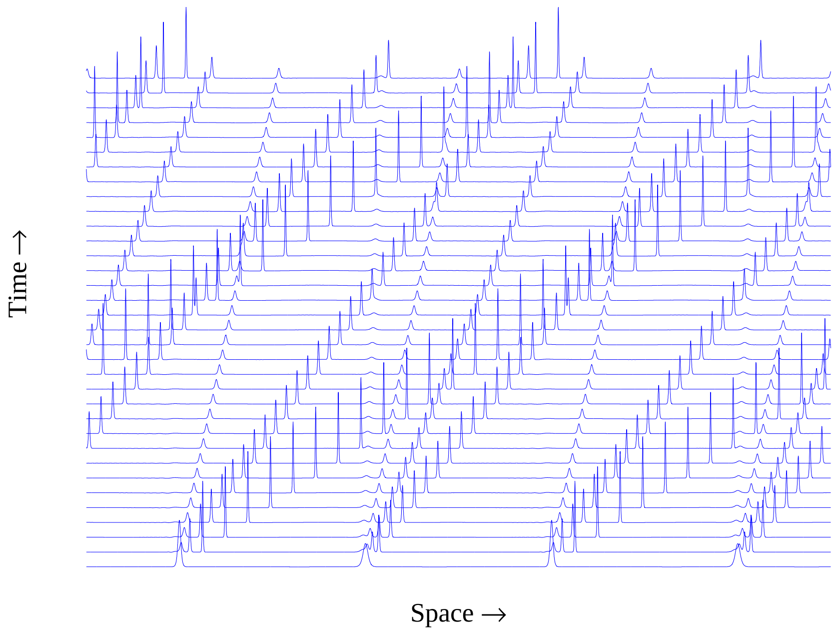

Fig. 4. Interactions of KdV soliton ensembles with weak tails. Timeslice plot over two space periods for $\alpha_1 = 1$, $\alpha_2 = 0.1$, $\beta = 111.11$, $0 \leq t \leq 100$, $A_1 = 8$, $A_2 = 4$.

In the present subsection we consider two sets of initial pulses: in the first case $A_1 = 8$ and $A_2 = 4$ ($\alpha_1 = 1$, $\alpha_2 = 0.1$, $\beta = 111.11$, see Figs. 4–6) and

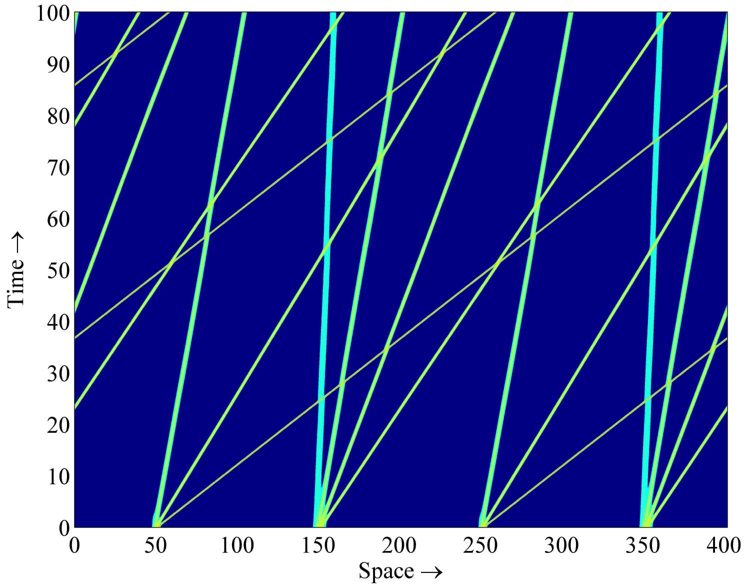

Fig. 5. Interactions of KdV soliton ensembles with weak tails. Pseudocolor plot over two space periods for $\alpha_1 = 1$, $\alpha_2 = 0.1$, $\beta = 111.11$, $0 \leq t \leq 100$, $A_1 = 8$, $A_2 = 4$.

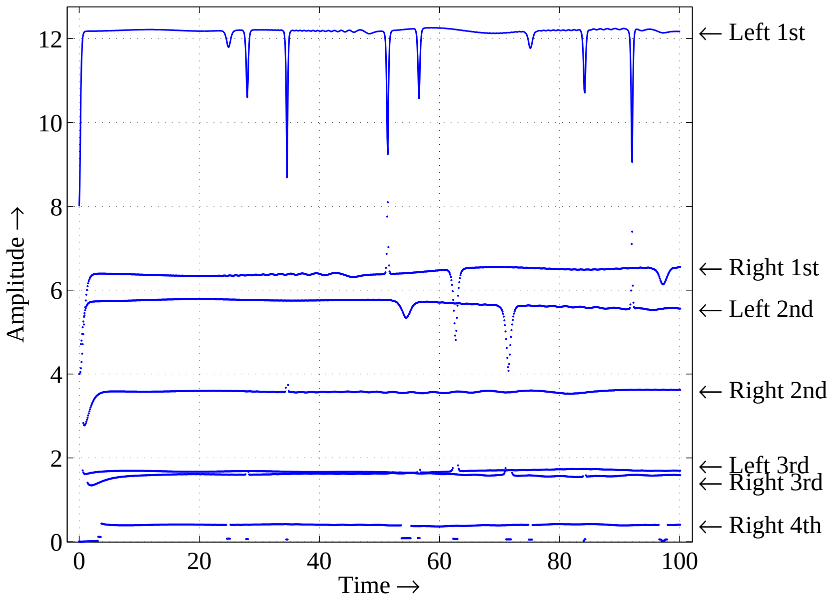

Fig. 6. Interactions of KdV soliton ensembles with weak tails. Wave-profile maxima against time in case of $\alpha_1 = 1$, $\alpha_2 = 0.1$, $\beta = 111.11$, $0 \leq t \leq 100$, $A_1 = 8$, $A_2 = 4$.

in the second case $A_1 = 15$ and $A_2 = 5$ ($\alpha_1 = 0.07$, $\alpha_2 = 0.03$, $\beta = 111.11$, see Figs. 7–9). In both cases two different soliton ensembles and (very) weak tails emerge from dual sech^2-type initial conditions. The number of solitons in the KdV soliton ensemble depends on the values of dispersion parameters α_1, α_2 and microstructure parameter β and on the value of the amplitude of the pulse A [1,18,19]. In the first case ensemble of three solitons emerge from the left hand side initial pulse and ensemble of four solitons form the right hand side pulse. In the second case the number of solitons in both ensembles is two. Emerged soliton ensembles are typical KdV soliton ensembles, i.e., the amplitude of the highest soliton in the KdV ensemble is always higher than the amplitude of the initial pulse. The tail is weak as it does not influence the behavior of the KdV ensemble greatly — it does not change the speed of solitons (see pseudocolor plots in Figs. 5 and 8), but it causes small oscillations in soliton amplitude curves (see Figs. 6 and 9).

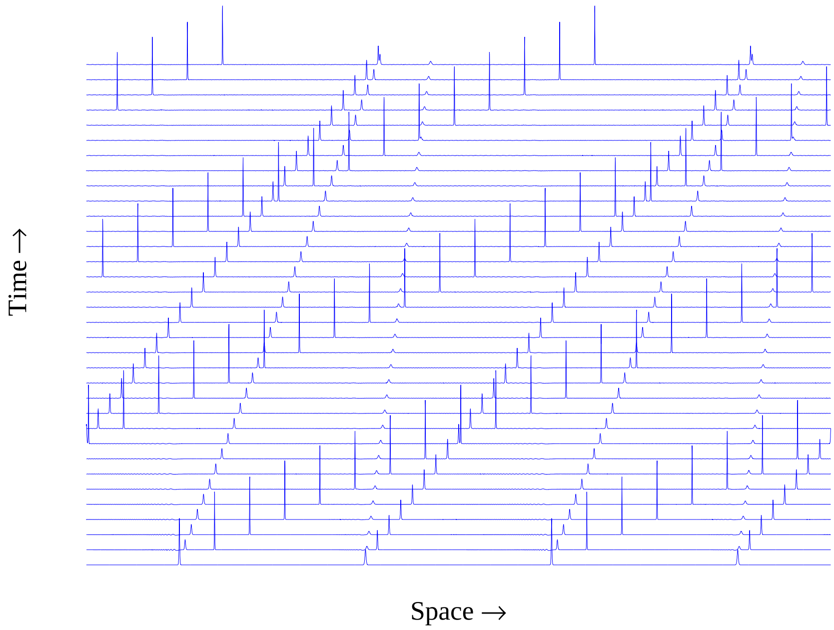

Fig. 7. Interactions of KdV soliton ensembles with weak tails. Timeslice plot over two space periods for $\alpha_1 = 0.07$, $\alpha_2 = 0.03$, $\beta = 111.11$, $0 \leq t \leq 100$, $A_1 = 15$, $A_2 = 5$.

Solitons with different amplitudes propagate at different speeds and therefore interactions between emerging solitons take place. One can trace here two type of interactions: (i) between solitons from different ensembles, and (ii) between solitons from the same ensemble. Both interaction types can be characterized as follows: (i) during interactions solitons are phase-shifted (Figs. 5 and 8) and amplitudes of higher solitons decrease (Figs. 6 and 9); (ii) after interactions solitons almost restore their amplitudes (Figs. 6 and 9) and speeds (Figs. 5 and 8). Besides the soliton-soliton interactions all solitons interact with tails. However, as the tails are weak, they does not influence the behaviour of solitons essentially and their influence can be traced only in curves of wave profile maxima, where tails can cause small oscillations. In conclusion, one can declare that observed interactions are nearly elastic and therefore solution can be called solitonic.

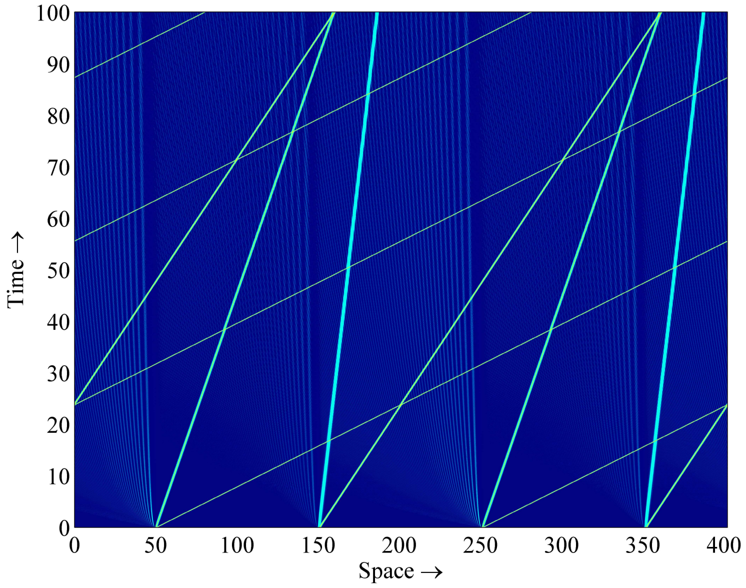

Fig. 8. Interactions of KdV soliton ensembles with weak tails. Pseudocolor plot over two space periods for $\alpha_1 = 0.07$, $\alpha_2 = 0.03$, $\beta = 111.1$, $0 \le t \le 100$, $A_1 = 15$, $A_2 = 5$.

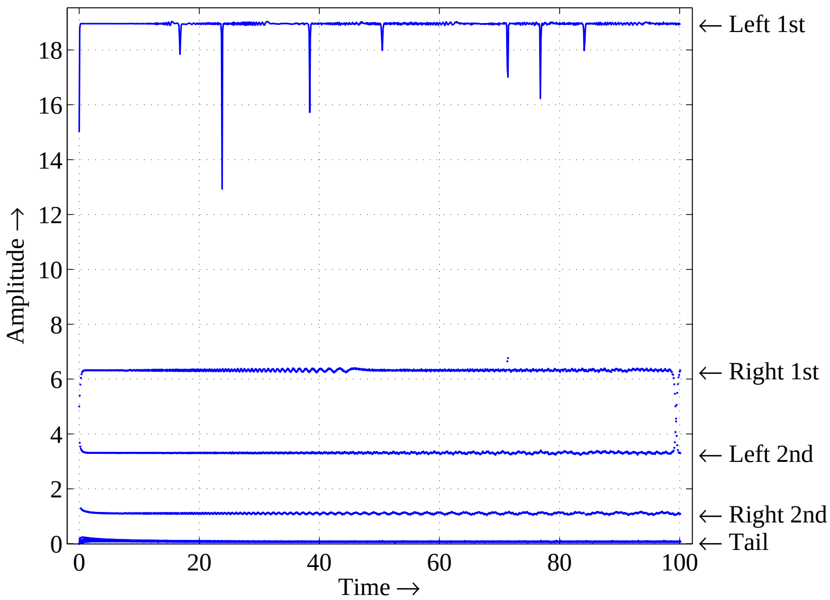

Fig. 9. Interactions of KdV soliton ensembles with weak tails. Wave-profile maxima against time in case of $\alpha_1 = 0.07$, $\alpha_2 = 0.03$, $\beta = 111.11$, $0 \le t \le 100$, $A_1 = 15$, $A_2 = 5$.

4.3 Interactions of solitons with strong tails

In the present case two solitons and strong tails emerge from the initial wave (2) (cf. the forth solution type in [1,18,19]). Due to different initial amplitudes emerged solitons propagate at different speed and therefore interact (see Figs. 10–12). For this solution type the tail is considered to be strong, because it influences the behavior of emerged solitary waves essentially: (i) amplitudes of the propagating solitary waves are lover than the amplitudes of the initial ones; (ii) amplitudes of propagating solitons are not constant, but due to the influence of tails they oscillate remarkably about a constant level (see Fig. 12). The decrease of the left and the right hand side solitary wave amplitudes is proportional to the initial amplitudes. In the example, considered here, propagating solitons are approximately 1.4 times lower than the initial waves. Such a phenomenon — shape of the initial wave is modified in a way to be more appropriate to the real solution of the equation — is called selection (see [28,29] for details).

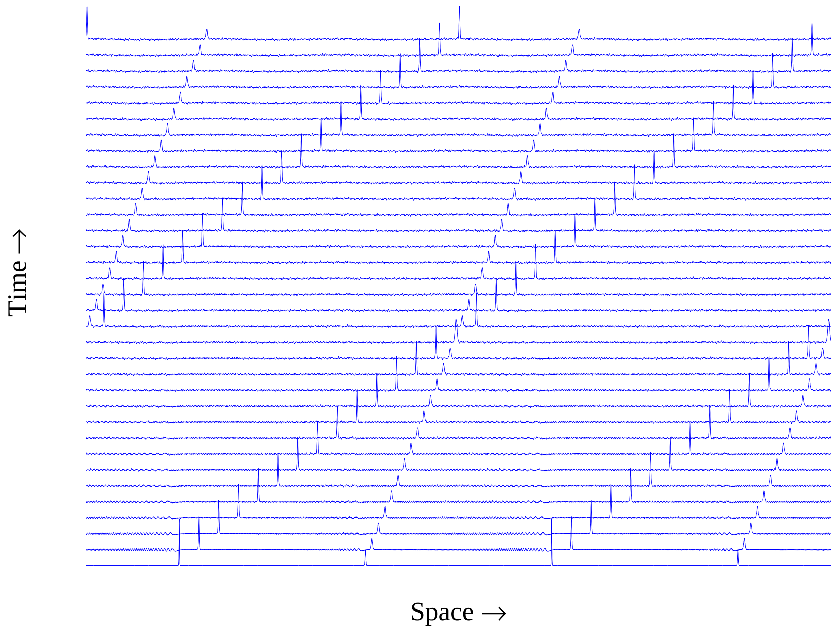

Fig. 10. Interactions of solitons with strong tails. Timeslice plot over two space periods for $\alpha_1 = 0.03$, $\alpha_2 = 0.07$, $\beta = 111.11$, $A_1 = 15$, $A_2 = 5$

The interaction produces phase shift in soliton trajectories — the higher solitary wave is shifted to the right and the lower amplitude solitary wave is shifted to the left. After the interaction both solitons almost restore their amplitudes. Therefore one can say, that the interaction is nearly elastic and the usage of term '(KdV) soliton' in our previous papers [1,18,19] is verified.

4.4 Interactions of solitary waves with tails and wave packets

The situation, discussed in the present subsection, corresponds to the fifth solution type in our previous papers [1,18,19]. In this case solitary waves, tails

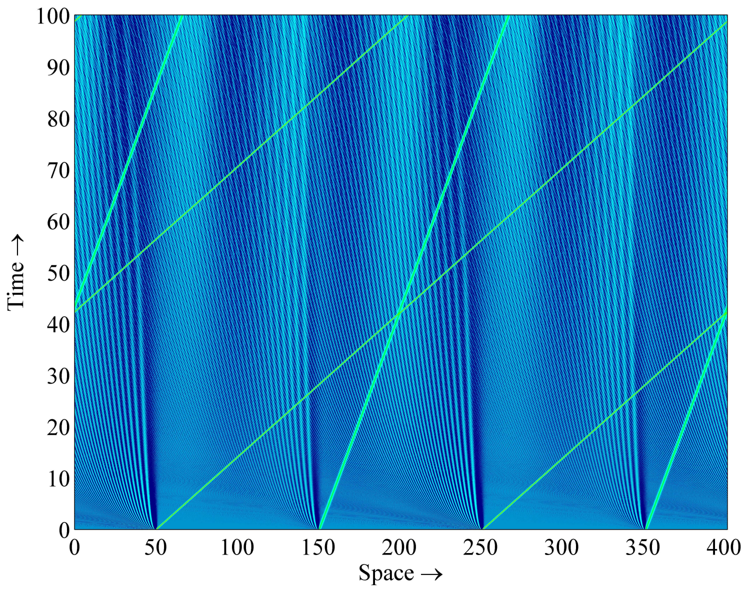

Fig. 11. Interactions of solitons with strong tails. Pseudocolor plot over two space periods for $\alpha_1 = 0.03$, $\alpha_2 = 0.07$, $\beta = 111.11$, $A_1 = 15$, $A_2 = 5$

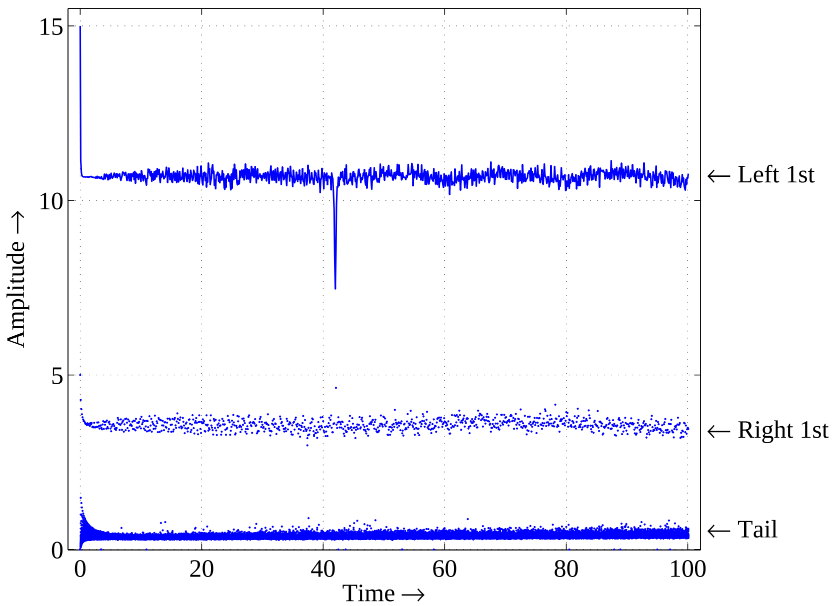

Fig. 12. Interactions of solitons with strong tails. Wave-profile maxima against time in case of $\alpha_1 = 0.03$, $\alpha_2 = 0.07$, $\beta = 111.11$, $0 \le t \le 100$, $A_1 = 15$, $A_2 = 5$.

and a wave packet (or several wave packets) emerge simultaneously. Christov and Velarde have described a similar solution type in [28]. Here we present four examples: in the first case $A_1 = 8$, $A_2 = 4$, $\alpha_1 = 0.05$, $\alpha_2 = 0.11$, and $\beta = 0.0111$ (see Figs. 13–16); in the second case $A_1 = 15$, $A_2 = 5$, $\alpha_1 = 0.05$, $\alpha_2 = 0.03$, and $\beta = 0.111$ (see Figs. 17–20); in the third case $A_1 = 8$, $A_2 = 4$, $\alpha_1 = 0.09$, $\alpha_2 = 0.11$, and $\beta = 0.0111$ (see Figs. 21–24); in the fourth case

$A_1 = 12$, $A_2 = 2$, $\alpha_1 = 0.09$, $\alpha_2 = 0.11$, and $\beta = 0.0111$ (see Figs. 25–28). All three components of the solution could be seen in timeslice plots in Figs. 13, 14, 17, 18, 21, 22, 25 and 26.

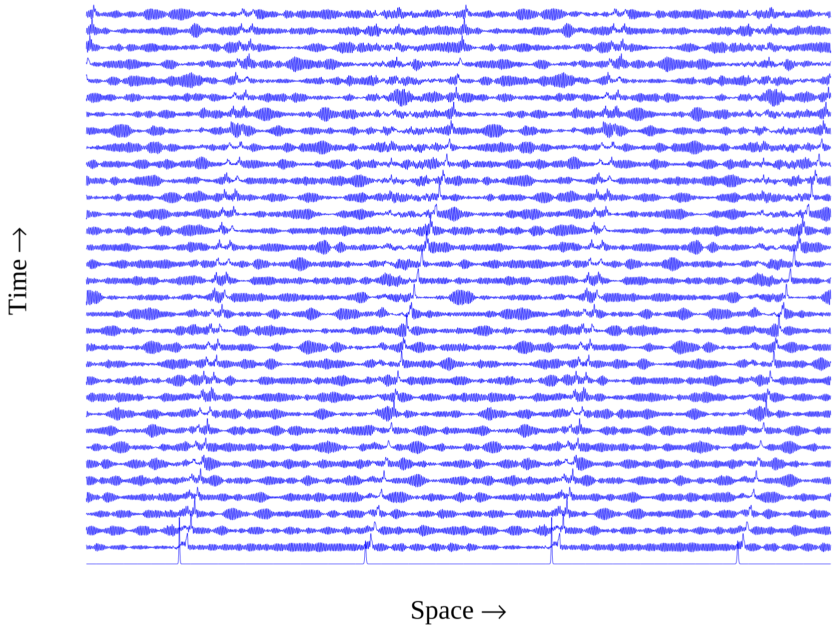

Fig. 13. Interactions of solitary waves with tails and wave packets. Timeslice plot over two space periods for $\alpha_1 = 0.05$, $\alpha_2 = 0.11$, $\beta = 0.0111$, $0 \leq t \leq 100$, $A_1 = 8$, $A_2 = 4$.

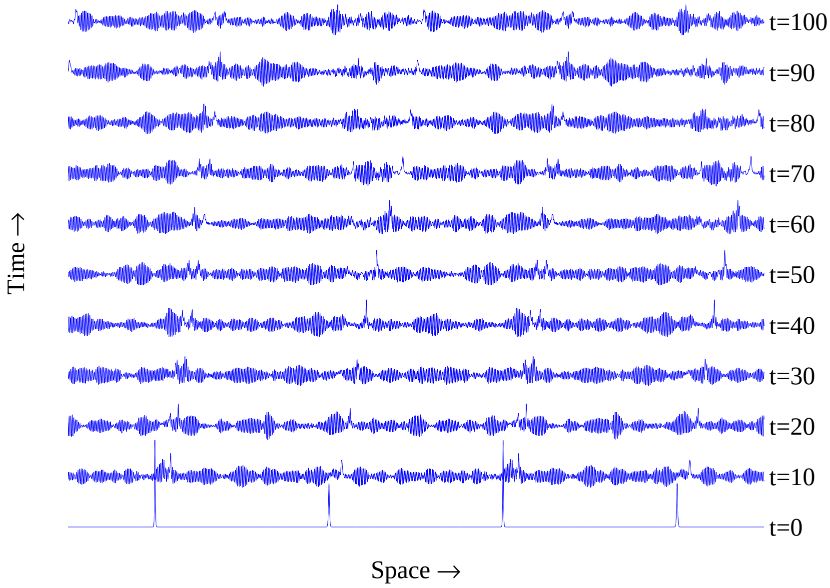

Fig. 14. Interactions of solitary waves with tails and wave packets. Single wave-profiles at $t = 0$, $t = 10$, $t = 20$, $t = 30$, $t = 40$, $t = 50$, $t = 60$, $t = 70$, $t = 80$, $t = 90$, $t = 100$ over two space periods for $\alpha_1 = 0.05$, $\alpha_2 = 0.11$, $\beta = 0.0111$, $0 \leq t \leq 100$, $A_1 = 8$, $A_2 = 4$.

Due to the complicated structure of the solution, different interactions can

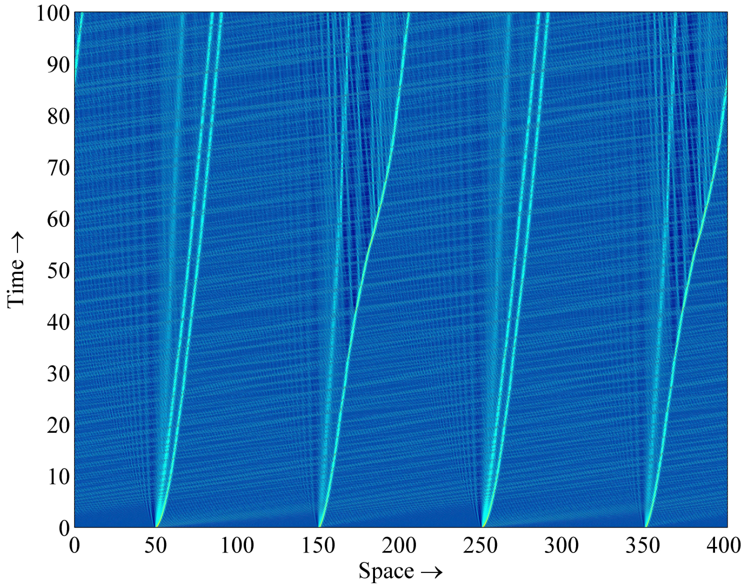

Fig. 15. Interactions of solitary waves with tails and wave packets. Pseudocolor plot over two space periods for $\alpha_1 = 0.05$, $\alpha_2 = 0.11$, $\beta = 0.0111$, $0 \le t \le 100$, $A_1 = 8$, $A_2 = 4$.

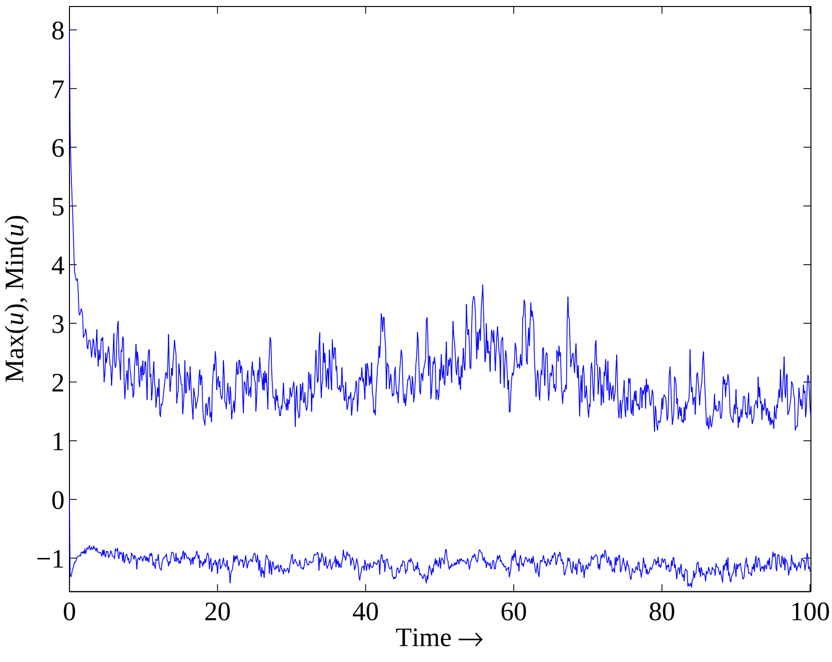

Fig. 16. Interactions of solitary waves with tails and wave packets. Wave-profile maximum and minimum against time in case of $\alpha_1 = 0.05$, $\alpha_2 = 0.11$, $\beta = 0.0111$, $0 \le t \le 100$, $A_1 = 8$, $A_2 = 4$.

take place: (i) solitary wave – solitary wave; (ii) solitary wave – tail; (iii) solitary wave – wave packet; (iv) tail – wave packet; (v) interactions between wave packets. In papers [1,19] we found that for all solution types the speed of solitary waves (solitons) depends on the amplitude of the initial wave — the higher the wave the higher its speed. Therefore we hoped that interacting solitary waves emerge from different amplitude initial waves for the present solution type. However, due to the emergence of different wave packets the situation here is more complicated than in the case of a single initial pulse. In the latter case besides the tail and wave packets only one solitary wave emerged. Now several solitary waves can be emerged from both initial pulses and interacting solitary waves were detected in few cases only. The influence of different wave packets on the behaviour of solitary waves can be so strong that their amplitudes decrease rapidly and it is practically impossible to distinguish between solitary waves and wave packets in time dependencies of wave profile maxima (Figs. 16 and 20). On the other hand, according to timeslice and pseudocolor plots in Figs. 13, 14, 15, 17, 18 and 19, emerged solitary waves are not completely suppressed. One can say, that a very strong selection procedure takes place and shapes of all solitary waves are altered to a certain critical amplitude level, which can be several times lower than the amplitude of the initial wave, see Figs. 16, 20, 24 and 28. In some cases, like the one presented in Figs. 21–24, the selection procedure is not so strong and it is easy to distinguish between solitary waves and wave packets. Due to the fact that all emerged solitary waves are selected to nearly the same amplitude level they all are propagating at nearly the same speed and do not interact, see Figs. 13, 19, 17, 19, 21 and 23. In few cases different solitary waves are selected to different amplitude levels and therefore interactions between solitary waves takes place. A corresponding example is presented in Figs. 25–28. However, it is clear that these interactions are not elastic — speeds of solitons are altered during interactions, see Figs. 25–27. Amplitudes of solitary waves oscillate strongly in all four cases due to interactions between solitary waves and wave packets, see Figs. 16, 20, 24 and 28.

Notwithstanding these different interactions and selection phenomenon, all three components of the solution are conserved over the whole integration time interval. In this sense the solution is stable. However, in the present case we cannot declare that emerged solitary waves are solitons, because either it is impossible to simulate interactions between solitary waves or interactions are not elastic.

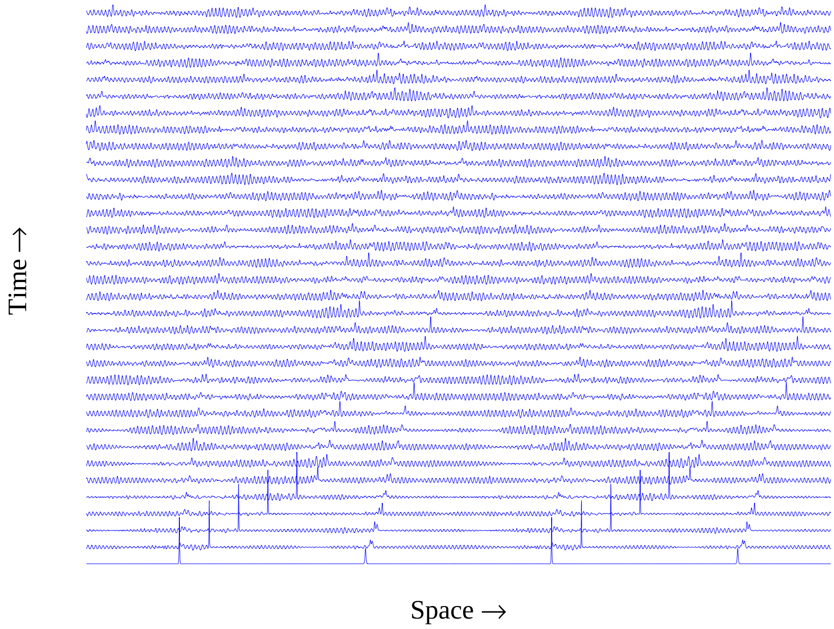

Fig. 17. Interactions of solitary waves with tails and wave packets. Timeslice plot over two space periods for $\alpha_1 = 0.05$, $\alpha_2 = 0.03$, $\beta = 0.111$, $0 \le t \le 100$, $A_1 = 15$, $A_2 = 5$.

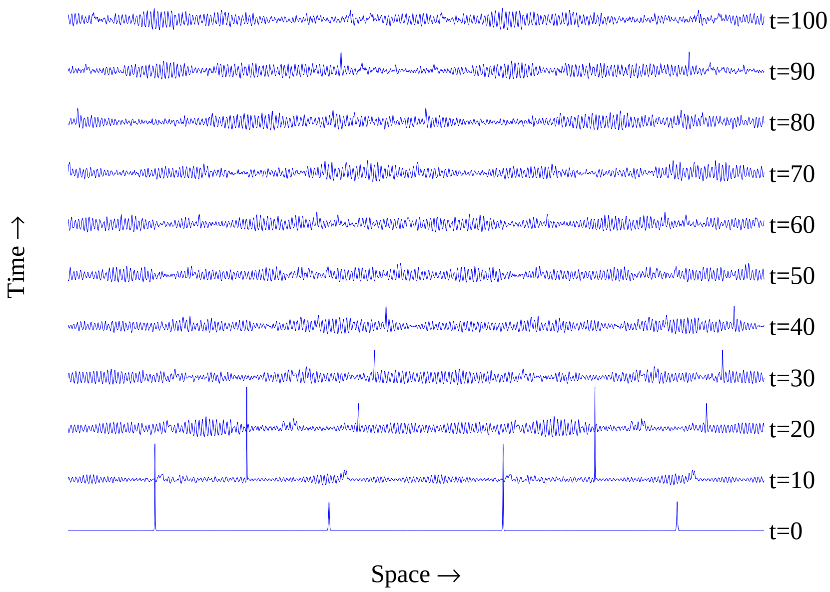

Fig. 18. Interactions of solitary waves with tails and wave packets. Single wave-profiles at $t = 0$, $t = 10$, $t = 20$, $t = 30$, $t = 40$, $t = 50$, $t = 60$, $t = 70$, $t = 80$, $t = 90$, $t = 100$ over two space periods for $\alpha_1 = 0.05$, $\alpha_2 = 0.03$, $\beta = 0.111$, $0 \le t \le 100$, $A_1 = 15$, $A_2 = 5$.

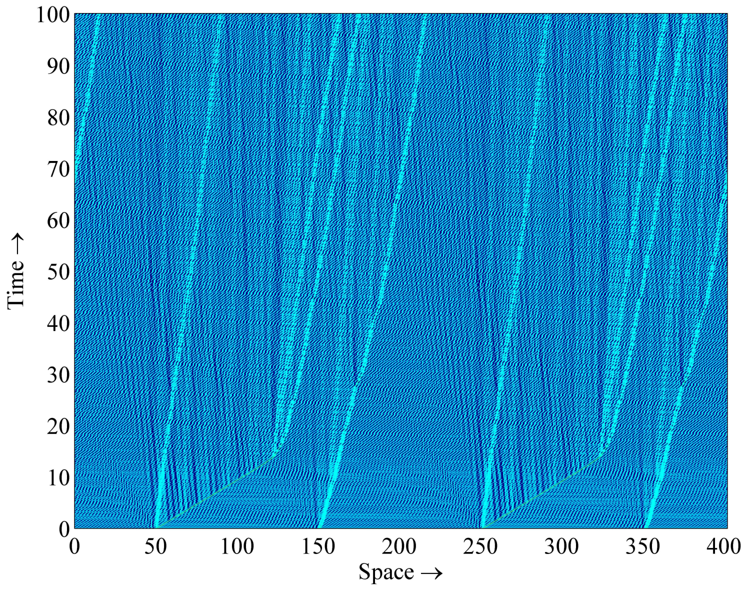

Fig. 19. Interactions of solitary waves with tails and wave packets. Pseudocolor plot over two space periods for $\alpha_1 = 0.05$, $\alpha_2 = 0.03$, $\beta = 0.111$, $0 \leq t \leq 100$, $A_1 = 15$, $A_2 = 5$.

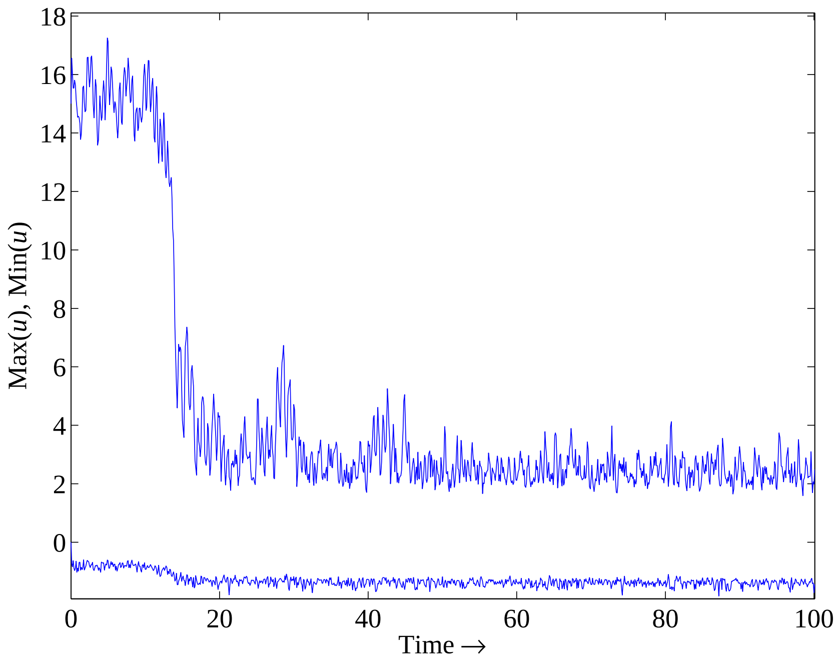

Fig. 20. Interactions of solitary waves with tails and wave packets. Wave-profile maximum and minimum against time in case of $\alpha_1 = 0.05$, $\alpha_2 = 0.03$, $\beta = 0.111$, $0 \leq t \leq 100$, $A_1 = 15$, $A_2 = 5$.

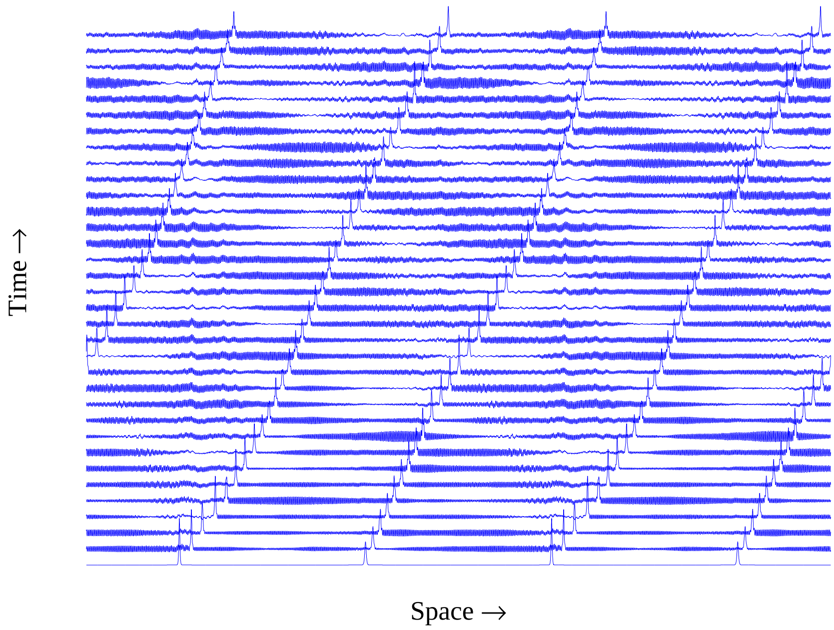

Fig. 21. Interactions of solitary waves with tails and wave packets. Timeslice plot over two space periods for $\alpha_1 = 0.09$, $\alpha_2 = 0.11$, $\beta = 0.0111$, $0 \leq t \leq 100$, $A_1 = 8$, $A_2 = 4$.

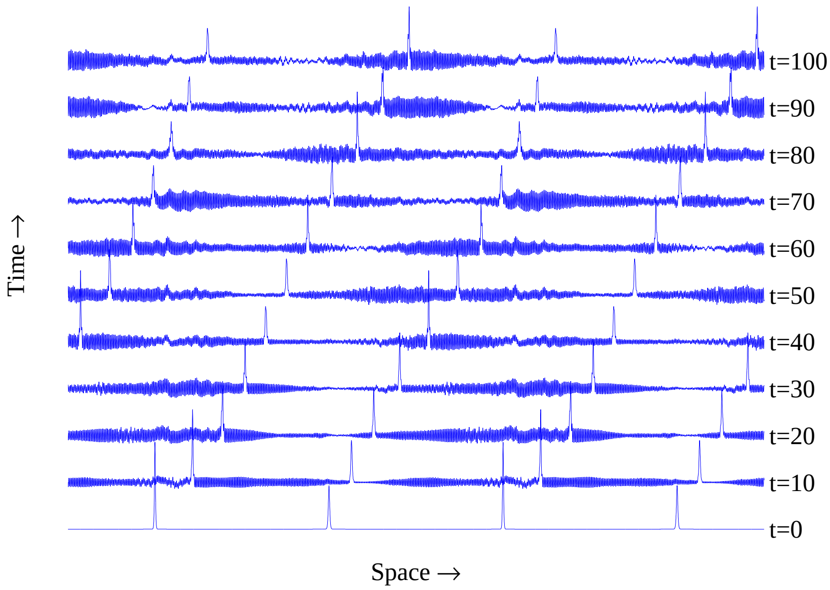

Fig. 22. Interactions of solitary waves with tails and wave packets. Single wave-profiles at $t = 0$, $t = 10$, $t = 20$, $t = 30$, $t = 40$, $t = 50$, $t = 60$, $t = 70$, $t = 80$, $t = 90$, $t = 100$ over two space periods for $\alpha_1 = 0.09$, $\alpha_2 = 0.11$, $\beta = 0.0111$, $0 \leq t \leq 100$, $A_1 = 8$, $A_2 = 4$.

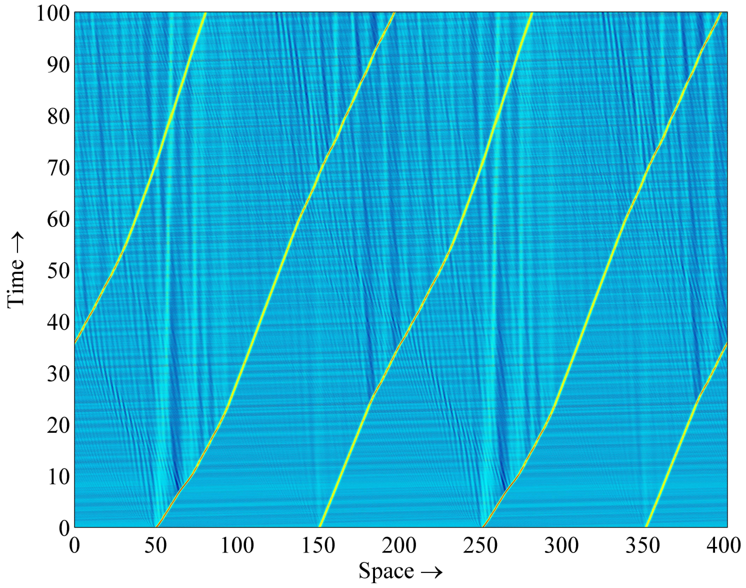

Fig. 23. Interactions of solitary waves with tails and wave packets. Pseudocolor plot over two space periods for $\alpha_1 = 0.09$, $\alpha_2 = 0.11$, $\beta = 0.0111$, $0 \leq t \leq 100$, $A_1 = 8$, $A_2 = 4$.

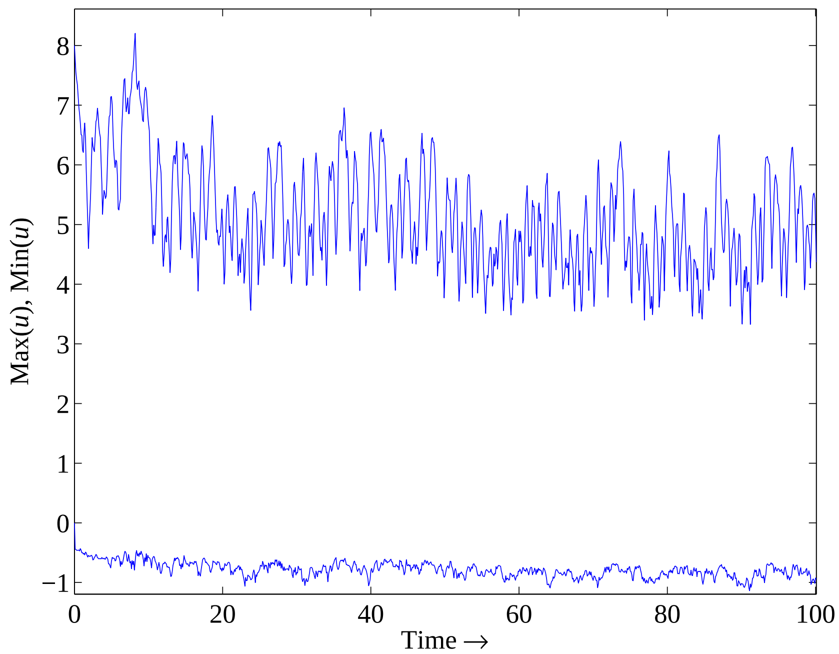

Fig. 24. Interactions of solitary waves with tails and wave packets. Wave-profile maximum and minimum against time in case of $\alpha_1 = 0.09$, $\alpha_2 = 0.11$, $\beta = 0.0111$, $0 \leq t \leq 100$, $A_1 = 8$, $A_2 = 4$.

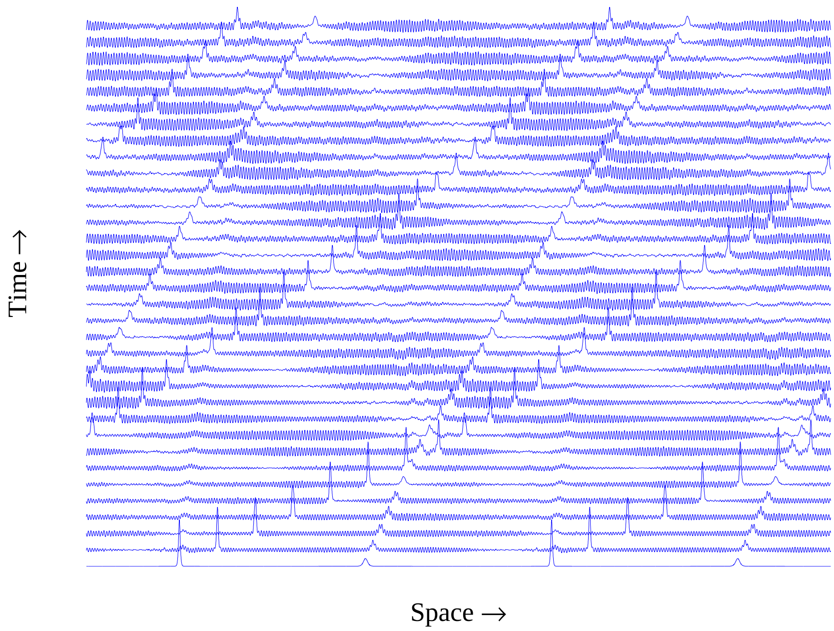

Fig. 25. Interactions of solitary waves with tails and wave packets. Timeslice plot over two space periods for $\alpha_1 = 0.09$, $\alpha_2 = 0.11$, $\beta = 0.0111$, $0 \leq t \leq 100$, $A_1 = 12$, $A_2 = 2$.

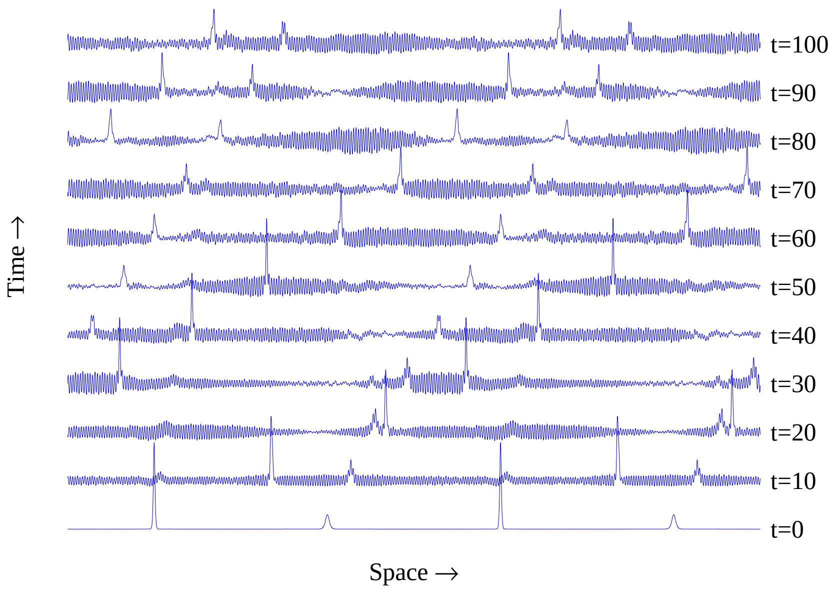

Fig. 26. Interactions of solitary waves with tails and wave packets. Single wave-profiles at $t = 0$, $t = 10$, $t = 20$, $t = 30$, $t = 40$, $t = 50$, $t = 60$, $t = 70$, $t = 80$, $t = 90$, $t = 100$ over two space periods for $\alpha_1 = 0.09$, $\alpha_2 = 0.11$, $\beta = 0.0111$, $0 \leq t \leq 100$, $A_1 = 12$, $A_2 = 2$.

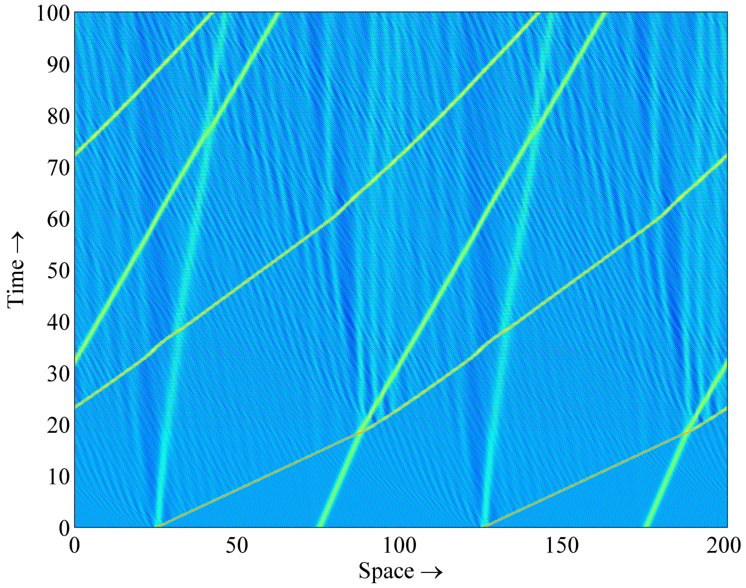

Fig. 27. Interactions of solitary waves with tails and wave packets. Pseudocolor plot over two space periods for $\alpha_1 = 0.09$, $\alpha_2 = 0.11$, $\beta = 0.0111$, $0 \le t \le 100$, $A_1 = 12$, $A_2 = 2$.

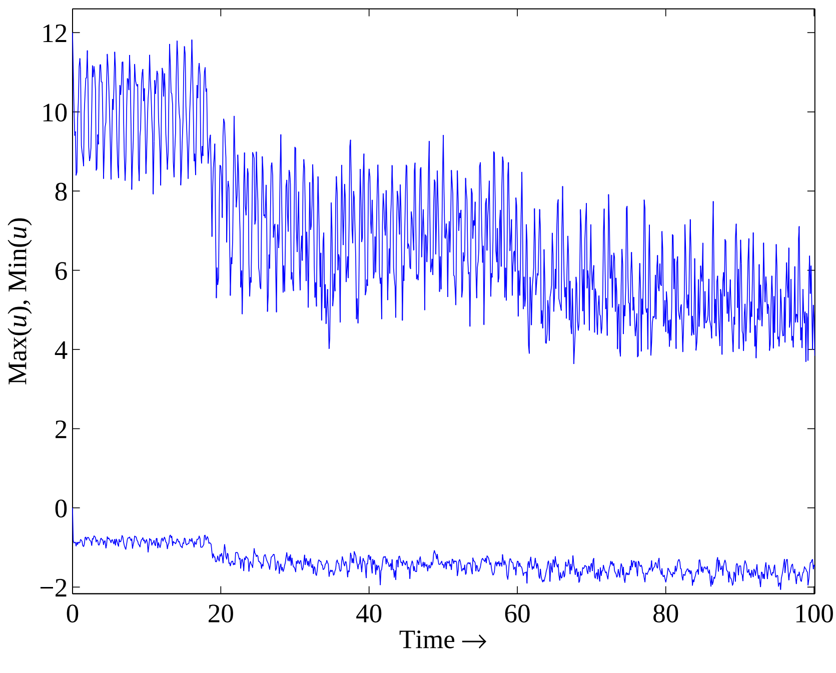

Fig. 28. Interactions of solitary waves with tails and wave packets. Wave-profile maximum and minimum against time in case of $\alpha_1 = 0.09$, $\alpha_2 = 0.11$, $\beta = 0.0111$, $0 \le t \le 100$, $A_1 = 12$, $A_2 = 2$.

In papers [1,19] we have described the phenomenon of the formation of wave packets in terms of time averaged spectral densities. If $U(k,t)$ is the DFT of function $u(x,t)$, defined by expression (3), then spectral densities

$$
\begin{aligned}
S(k,t) &= \frac{4\left(U(k,t)\right)^2}{n^2}, \quad k = 1, ..., \frac{n}{2} - 1, \\
S(k,t) &= \frac{2\left(U(k,t)\right)^2}{n^2}, \quad k = \frac{n}{2}.
\end{aligned}
\tag{14}
$$

For each value of t one can define the sum of spectral densities

$$
S_{sum}(t) = \sum_{k=1}^{n/2} S(k,t), \tag{15}
$$

normalised spectral densities

$$
S_{norm}(k,t) = \frac{S(k,t)}{S_{sum}(t)} \cdot 100\% \tag{16}
$$

and time averaged normalised spectral densities (TANSD)

$$
S_a(k,t) = \frac{\int_0^t S_{norm}(k,t)dt}{t}. \tag{17}
$$

We have discrete values of spectral densities S and S_{norm} at discrete time moments t_i, i.e. we have $S(k,t_i)$ and $S_{norm}(k,t_i)$. Therefore at $t = t_k$

$$
S_a(k,t_k) = \frac{\sum_{i=1}^k S_{norm}(k,t_i)}{k}. \tag{18}
$$

TANSD (18) reflect the contribution of the k-th spectral density (or amplitude) over the time interval $[0,t_k]$. Compared with spectral densities (or amplitudes) TANSD curves give more clear understanding about domination of certain harmonics. The idea of applying time averaged normalised spectral densities comes from [30] where "time average energies of single modes" are used in order to discuss the energy equipartition in systems of FPU type.

In Fig. 29 TANSD are presented for $\alpha_1 = 0.05$, $\alpha_2 = 0.11$, $\beta = 0.0111$, $A_1 = 8$, $A_2 = 4$ and in Fig. 30 for $\alpha_1 = 0.05$, $\alpha_2 = 0.03$, $\beta = 0.111$, $A_1 = 15$, $A_2 = 5$ (see corresponding timeslice plots in Figs. 13 and 17).

It is clear that wave packets are formed by amplified higher order harmonics and the $S_{\mathrm{a}}(k,t)$ having the highest value determines the number of maxima (oscillations) in a given wave profile. Similar situations are described in many textbooks (see e.g. [31]) in order to explain group velocity and dispersion phenomena — a sum of harmonic waves having nearly equal frequencies presents a wave packet. In the present case the envelope of the packet can propagate

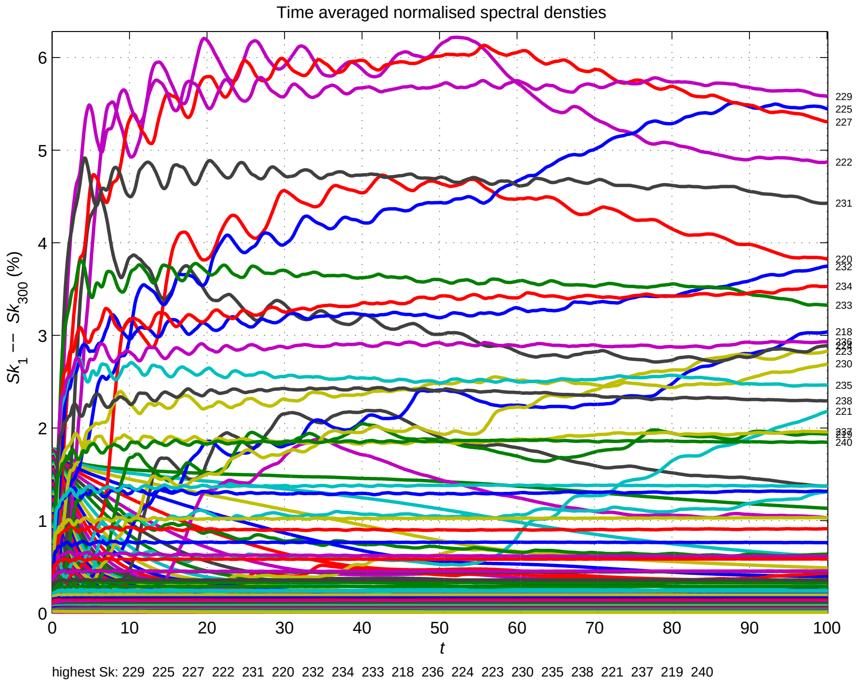

Fig. 29. Interactions of solitary waves with tails and wave packets. Time averaged spectral densities plot $\alpha_1 = 0.05$, $\alpha_2 = 0.11$, $\beta = 0.0111$, $n = 4096$, $t_f = 100$, $A_1 = 8$, $A = 4$.

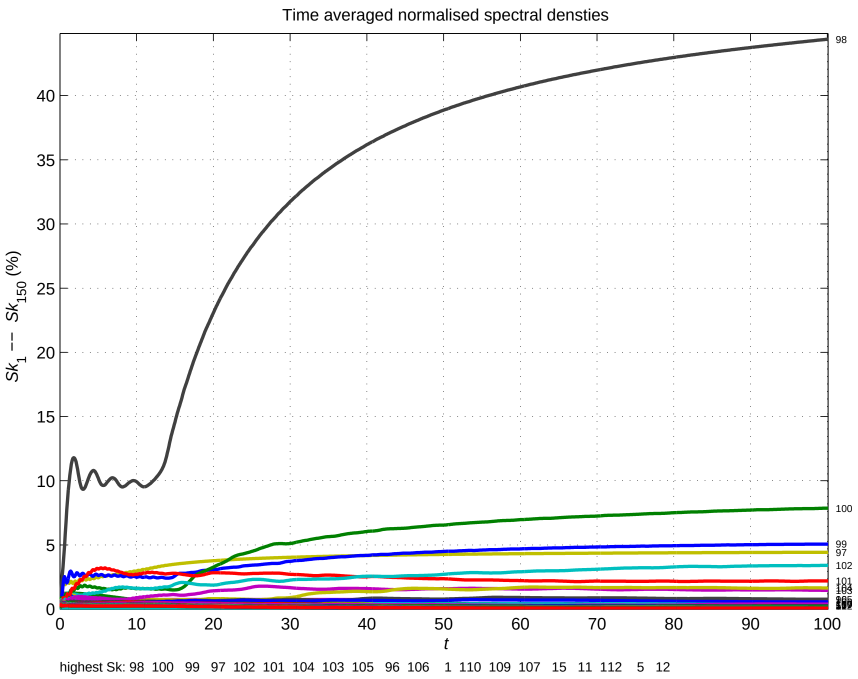

Fig. 30. Interactions of solitary waves with tails and wave packets. Time averaged spectral densities plot $\alpha_1 = 0.05$, $\alpha_2 = 0.03$, $\beta = 0.111$, $n = 4096$, $t_f = 100$, $A_1 = 15$, $A = 5$.

to the left or to the right and at much higher speed than that of the emerged solitary waves or high frequency waves that form the packet. One can conclude that in Fig. 29 $S_a(k,t)$ for $218 \leq k \leq 240$ and in Fig. 30 for $97 \leq k \leq 102$ are amplified and therefore generate wave packets.

The wave packets that are formed in the present case are slightly different from the case described in [1,19]. In the present case there are two sets of different wave packets, one formed from the left-hand and the another formed from the right-hand initial pulse. Based on the analysis in [1,19] one can say that, the shape of the wave packet depends on the amplitude of the initial excitation. Having two pulses of different amplitudes in the initial excitation two interacting sets of wave packets are generated. In the present case the number of amplified harmonics are much higher than the number amplified harmonics in the case of single sech^2 initial condition described in [1,18,19]. The contribution of amplified harmonics is significant and they dominate over the lower harmonics.

Based on the given examples, one can say, that the wave packets influence the propagation of the solitary waves essentially:

(1) In the first (Figs. 13–16) and in the second case (Figs. 17–20) initial solitary waves can be decomposed into several solitary waves, which have amplitudes much less than the amplitudes of initial waves. In some cases the amplitudes of emerged solitary waves are so low that it is complicated to distinguish between solitary waves and wave packets in single profiles (Figs. 14 and 18) However in timeslice plots (Figs. 13 and 17) and pseudocolourplots (Figs. 15 and 19) trajectories of solitary waves can be traced.
(2) In the third case, in Figs. 21–24, the amplitude of the higher solitary wave decreases and that of the lower solitary wave increases to nearly equal level in the beginning of the integration interval. Later the solitary wave “change their amplitudes (and speeds)” two times. In other words, between $t \approx 25$ and $t \approx 55$ the right solitary wave is higher than the left one and for $t > 55$ the left solitary wave is again higher and faster. However, no interactions take place.
(3) In the fourth case, in Figs. 25–28, the shape and speed of the solitary waves are altered after the interaction , i.e. the interaction is not elastic.

5 Conclusions

In the present paper interactions of solitary waves in media governed by HKdV equation (1) are examined. The model equation is integrated numerically under initial condition (2) and periodic boundary condition (13). The solitonic character of interactions is examined in all considered cased:

- In cases of single KdV solitons, KdV soliton ensembles with weak tails and solitons with strong tails interactions are found to be elastic or nearly elastic. Therefore in these cases emerged solitary waves can be called solitons.
- In case of solitary waves with tails and wave packets (i) interacting solitary waves emerge only in few cases, and (ii) if interactions takes place then they are not elastic by means of solitons. Therefore these solitary waves cannot be called as solitons.

Acknowledgments

Authors of this paper thank Professor Jüri Engelbrecht for helpful discussions and senior researcher Pearu Peterson for Python related scientific software developments and assistance. The research was partially supported by Estonian Science Foundation Grant No 7035 (A.S. and L.I.) and EU Marie Curie Transfer of Knowledge project MTKD-CT-2004-013909 under FP 6 (A.S.).

References

[1] L. Ilison, A. Salupere, Propagation of sech^2-type solitary waves in hierarchical KdV-type systems, Mathematics and Computers in Simulation (submitted).

[2] G. Maugin, Nonlinear Waves in Elastic Crystals, Oxford Univ. Press, Oxford, 1999.

[3] V. I. Erofeev, Wave Processes in Solids with Microstructure, World Scientific, Singapore, 2003.

[4] J. Engelbrecht, A. Berezovski, F. Pastrone, M. Braun, Waves in microstructured materials and dispersion, Phil. Mag. 85 (2005) 4127–4141.

[5] P. Giovine, F. Oliveri, Dynamics and wave propagation in dilatant granular materials, Meccanica 30 (1995) 341–357.

[6] F. Oliveri, Wave propagation in granular materials as continua with microstructure: Application to seismic waves in a sediment filled site, Rendiconti Circolo Matematico di Palermo 45 (1996) 487–499.

[7] G. Cataldo, F. Oliveri, Nonlinear seismic waves: A model for site effects, Int. J. Non-linear Mech. 34 (1999) 457–468.

[8] F. Oliveri, M. P. Speciale, Wave hierarchies in continua with scalar microstructure in the plane and spherical symmetry, Computers and Mathematics with Applications 55 (2008) 285–298.

[9] G. Whitham, Linear and Nonlinear Waves, John Wiley & Sons, New York, 1974.

[10] Y. Zhu, Q. Chang, S. Wu, Exact solitary-wave solutions with compact support for the modified KdV equation, Chaos, Solitons & Fractals 24 (2005) 365–369.

[11] C. Dai, J. Zhu, J. Zhang, New exact solutions to the mKdV equation with variable coefficients, Chaos, Solitons & Fractals 27 (2006) 881–886.

[12] R. Wu, J. Sun, Soliton-like solutions to the GKdV equation by extended mapping method, Chaos, Solitons & Fractals 31 (2007) 70–74.

[13] Y. Zhang, D.-Y. Chen, A new representation of N-soliton solution and limiting solutions for the fifth order KdV equation, Chaos, Solitons & Fractals 23 (2005) 1055–1061.

[14] Y. Zhang, D.-Y. Chen, Z.-B. Li, A direct method for deriving a multisoliton solution to the fifth order KdV equation, Chaos, Solitons & Fractals 29 (2006) 1188–1193.

[15] O. Ilison, A. Salupere, Propagation of sech^2-type solitary waves in higher order KdV-type systems, Chaos, Solitons & Fractals 26 (2005) 453–465.

[16] O. Ilison, A. Salupere, On the propagation of solitary pulses in microstructured materials, Chaos, Solitons & Fractals 29 (2006) 202–214.

[17] M. A. Helal, M. S. Mehanna, A comparative study between two different methods for solving the general Korteweg–de Vries equation (GKdV), Chaos, Solitons & Fractals 33 (2007) 725–739.

[18] L. Ilison, A. Salupere, P. Peterson, On the propagation of localised perturbations in media with microstructure, Proc. Estonian Acad. Sci. Phys. Math. 56 (2) (2007) 84–92.

[19] L. Ilison, A. Salupere, Propagation of localised perturbations in granular materials, Research Report Mech 287/07, Institute of Cybernetics at Tallinn University of Technology (2007).

[20] H.-O. Kreiss, J. Oliger, Comparison of accurate methods for the integration of hyperbolic equations, Tellus 30 (1972) 341–357.

[21] A. Salupere, On the application of the pseudospectral method for solving the Korteweg–de Vries equation, Proc. Estonian Acad. Sci. Phys. Math. 44 (1) (1995) 73–87.

[22] A. Salupere, On the application of pseudospectral methods for solving nonlinear evolution equations, and discrete spectral analysis, in: Proc. of 10th Nordic Seminar on Computational Mechanics, Tallinn, TTU, 1997, pp. 76–83.

[23] B. Fornberg, Practical Guide to Pseudospectral Methods, Cambridge University Press, 1998.

[24] E. Jones, T. Oliphant, P. Peterson, et al., SciPy: Open source scientific tools for Python, http://www.scipy.org (2007).

[25] M. Frigo, S. G. Johnson, The design and implementation of FFTW3, Proceedings of the IEEE 93 (2) (2005) 216–231.

[26] P. Peterson, F2PY: Fortran to Python interface generator, http://cens.ioc.ee/projects/f2py2e/ (2005).

[27] A. C. Hindmarsh, Odepack, a systematized collection of ODE solvers, in: R. S. Stepleman, et al. (Eds.), Scientific Computing, North-Holland, Amsterdam, 1983, pp. 55–64.

[28] C. Christov, M. Velarde, Dissipative solitons, Physica D 86 (1995) 323–347.

[29] A. V. Porubov, Amplification of Nonlinear Strain Waves in Solids, World Scientific, Singapore, 2003.

[30] L. Galgani, A. Giorgilli, A. Martinoli, S. Vanzini, On the problem of energy equipartition for large systems of the Fermi–Pasta–Ulam type: analytical and numerical estimates, Physica D 59 (1992) 334–348.

[31] J. Billingham, A. King, Wave Motion, Cambridge University Press, Cambridge et al., 2000.